Rapid Communications

Skyrmion mass from spin-phonon interaction

D. Capic, E. M. Chudnovsky, and D. A. Garanin

Physics Department, Herbert H. Lehman College and Graduate School, The City University of New York, 250 Bedford Park Boulevard West, Bronx, New York 10468-1589, USA

(Received 20 May 2020; accepted 29 July 2020; published 10 August 2020)

The inertial mass of a skyrmion arising from spin-phonon interaction is computed exactly within a toy model of the magnetoelastic coupling in a ferromagnetic film. The mass scales as the square of the strength of the magnetoelastic coupling, as the square of the film thickness, and as the first power of the lateral size of the skyrmion. For nanometer skyrmions it is in the ballpark of a few electron masses but may be significantly greater in materials with large magnetostriction. These findings are expected to stand for any complex structure of spin-phonon interaction in real materials. They must be taken into account when addressing the speed of information processing based upon skyrmions.

DOI: 10.1103/PhysRevB.102.060404

Magnetic skyrmions are swirls of magnetization in thin films. They proliferated into condensed matter physics [1–7] from field models of atomic nuclei and topologically stable elementary particles [8–12]. In ferro- and antiferromagnets they are topological defects of the uniform magnetization (Néel vector) that cannot be easily destroyed. Unlike micron-size magnetic bubbles studied in the past [13,14], skyrmions can be small compared to the domain wall thickness, making them promising candidates for topologically protected nanoscale information processing [15–20].

Skyrmions can be moved by current-induced spin-orbit torques [20–23]. The speed of the information processing with skyrmions depends on their inertia. The effort to compute and measure skyrmion inertial mass has been limited so far. The mass of a skyrmion bubble of dipolar origin, similar to the Döring mass [24] of the domain wall in the thin-wall approximation, has been discussed by Makhfudz *et al.* [25]. Large inertia has been reported in experiments on skyrmion breathing modes in the gigahertz frequency range [26]. Similar effects have been observed in the breathing and hypocycloid motion of skyrmions by Shiino *et al.* [27]. Inertial mass of electromagnetic origin due to excitation of magnons by a moving skyrmion has been studied by Lin [28]. Psaroudaki *et al.* [29] have demonstrated that translational symmetry makes classical skyrmions massless. They computed the mass arising from defects, nonuniformity of the magnetic field, and confining potentials, and elucidated the contribution of thermal and quantum fluctuations to the mass. Kravchuk *et al.* [30] used collective coordinates to demonstrate that skyrmion dynamics in a continuous spin-field model is massless even if one accounts for magnon excitations. Massive skyrmions have been reported by Li *et al.* [31] in simulations of collective magnetic dynamics on a two-dimensional honeycomb lattice. Measurement of the mass of the oscillating skyrmion in a confined geometry of a semicircular nanoring has been recently proposed by Liu and Liang [32].

The range for the skyrmion mass obtained in experiments is rather broad. It is not always clear whether it is associated with the confined geometry or more fundamental effects studied by theorists. The latter hints towards zero skyrmion mass in the presence of full translational invariance. The crystal lattice violates such invariance. In this Rapid Communication we show that skyrmions acquire a finite mass due to the spin-phonon interaction even within translationally invariant continuous spin-field and elastic theories. The physics behind the contribution of the atomic lattice to the skyrmion mass is transparent. The time-dependent spin field corresponding to the moving skyrmion induces, through the magnetoelastic coupling, the motion of the atoms whose inertia contributes to the mass of the skyrmion. Materials that host skyrmions are rather complex. In addition to the dominant exchange interaction, they possess various other kinds of magnetic interactions that are important for stabilization of skyrmions, such as Dzyaloshinskii-Moriya, Zeeman, and crystal-field interactions [5,18,33–35]. Pertinent to our purpose, we shall consider in this Rapid Communication a toy model of the Belavin-Polyakov skyrmion [1] interacting with an isotropic elastic environment. We shall study two simple forms of the magnetoelastic coupling: The extreme anisotropic case and the fully isotropic case. The skyrmion is modeled by the dimensionless three-component spin field $\mathbf{S}$ of unit length given by [1]

$$S_x = \frac{2\lambda(x\cos\gamma - y\sin\gamma)}{\lambda^2 + x^2 + y^2}, \quad S_y = \frac{2\lambda(x\sin\gamma + y\cos\gamma)}{\lambda^2 + x^2 + y^2},$$
$$S_z = \frac{\lambda^2 - x^2 - y^2}{\lambda^2 + x^2 + y^2}, \quad \mathbf{S}^2 = S_x^2 + S_y^2 + S_z^2 = 1, \tag{1}$$

confined to the xy layer of thickness d, with $\mathbf{S}$ looking down at infinity. Here λ can be viewed as the lateral size of the skyrmion and γ describes the rotation of the spin field, with $\gamma = 0, \pi$ and $\gamma = \pm\pi/2$ corresponding to the Néel-type and Bloch-type skyrmions, respectively (see, e.g., Ref. [36]). Such a spin field is typical for nanometer-size skyrmions whose shape is dominated by the exchange interaction. The magnetoelastic interaction, which is weaker by orders of magnitude,

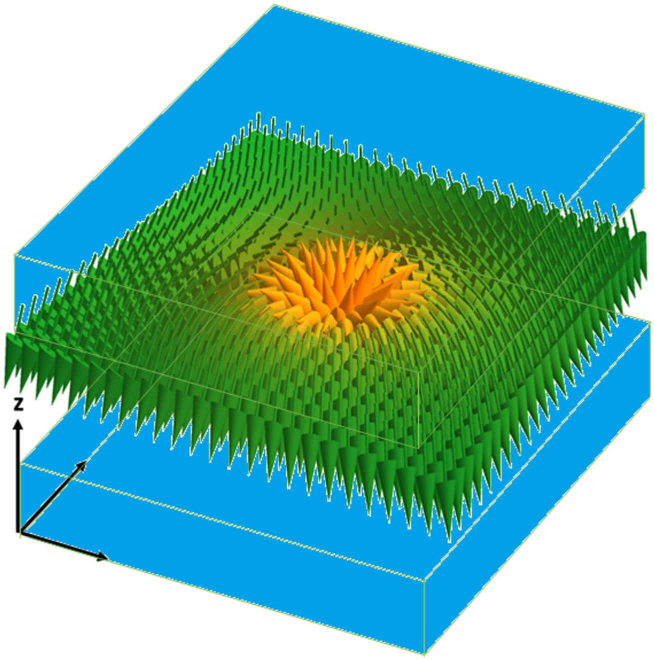

FIG. 1. Skyrmion in a magnetic layer confined between two nonmagnetic solids. Arrows show directions of the magnetization.

would generally be of the form $A_{ikjl}u_{ik}S_jS_l$, where

$$u_{ik} = \frac{1}{2}\left(\frac{\partial u_i}{\partial r_k} + \frac{\partial u_k}{\partial r_i}\right) \tag{2}$$

is the strain tensor, $\mathbf{u}$ is the phonon displacement field, and tensor A_{ikjl} represents components of the magnetoelastic energy density.

We shall start with the extreme anisotropic form of the magnetoelastic coupling, $Au_{zz}S_z^2$, that together with the elastic contribution yields for the energy

$$E = \int d^3r\left[\frac{1}{2}\rho\left(\frac{\partial \mathbf{u}}{\partial t}\right)^2 + \mu\left(u_{ik}^2 + \frac{\sigma}{1-2\sigma}u_{ll}^2\right) + Au_{zz}S_z^2\right]. \tag{3}$$

To simplify the problem we assume that the magnetic layer is confined between two nonmagnetic semi-infinite solids (see Fig. 1) having the same mass density ρ, the same shear modulus $\mu > 0$, and the same Poisson coefficient $\sigma = E/(2\mu) - 1$ (satisfying $-1 \leqslant \sigma \leqslant 1/2$), with E being the Young's modulus [37]. If the speed of the moving skyrmion is small compared to the speed of sound, the elastic deformation adiabatically follows the skyrmion via an extremal equation for the energy:

$$\nabla^2\mathbf{u} + \frac{1}{1-2\sigma}\nabla(\nabla\cdot\mathbf{u}) = -\frac{A}{\mu}\frac{\partial S_z^2}{\partial z}\mathbf{e}_z, \tag{4}$$

where $\mathbf{e}_z$ is the unit vector along the z axis. Its solution is

$$u_i(\mathbf{r}) = -\frac{A}{\mu}\int d^3r' G_{iz}(\mathbf{r}-\mathbf{r}')\left(\partial S_z^2/\partial z\right), \tag{5}$$

where

$$G_{ik} = \frac{1}{4\pi}\left[\frac{\delta_{ik}}{r} - \frac{1}{4(1-\sigma)}\frac{\partial^2 r}{\partial r_i \partial r_k}\right] \tag{6}$$

is the Green's function [37] of Eq. (4).

If the skyrmion moves along the x axis at a speed v the solution (5) must be replaced with $\mathbf{u}(x - vt, y, z)$. Its substitution into the first term of Eq. (3) gives for the kinetic energy, $E_k = \frac{1}{2}M_S v^2$, where

$$M_S = \rho\int d^3r\left(\frac{\partial \mathbf{u}}{\partial x}\right)^2 \tag{7}$$

is the mass of the skyrmion due to spin-phonon coupling. Substitution of Eq. (5) in the expression for the mass yields

$$M_S = \rho\left(\frac{A}{\mu}\right)^2\int d^3r'\int d^3r'' F_{zz}(\mathbf{r}'-\mathbf{r}'')\frac{\partial S_z^2(\mathbf{r}')}{\partial z'}\frac{\partial S_z^2(\mathbf{r}'')}{\partial z''}, \tag{8}$$

where

$$F_{zz}(\mathbf{r}'-\mathbf{r}'') = \frac{\partial}{\partial x'}\frac{\partial}{\partial x''}\int d^3r\, G_{iz}(\mathbf{r}-\mathbf{r}')G_{iz}(\mathbf{r}-\mathbf{r}''). \tag{9}$$

Using the Fourier transform of the Green's function (6),

$$G_{ik}(k) = \frac{1}{k^2}\left[\delta_{ik} - \frac{1}{2(1-\sigma)}\frac{k_i k_k}{k^2}\right], \tag{10}$$

F_{zz} can be written as

$$F_{kj}(\mathbf{r}'-\mathbf{r}'') = \int\frac{d^3k}{(2\pi)^3}e^{-i\mathbf{k}(\mathbf{r}'-\mathbf{r}'')}\frac{k_x^2}{k^4}\left[\delta_{kj} - p\frac{k_k k_j}{k^2}\right], \tag{11}$$

where

$$p = \frac{1}{(1-\sigma)}\left[1 - \frac{1}{4(1-\sigma)}\right] \tag{12}$$

is the parameter of the elastic theory satisfying $7/16 \leqslant p \leqslant 1$.

At this point it suffices to consider a thin-film approximation, $d \ll \lambda$, where one can write

$$S_z^2(\mathbf{r}) = S_z^2(\boldsymbol{\rho})d\delta(z) \tag{13}$$

with $\boldsymbol{\rho} = x\mathbf{e}_x + y\mathbf{e}_y$ being the radius vector in the xy plane of the magnetic layer. Integrating by parts in Eq. (8) one obtains

$$M_S = \rho\left(\frac{A}{\mu}\right)^2 d^2\int d^2\rho'\int d^2\rho'' K(\boldsymbol{\rho}'-\boldsymbol{\rho}'')S_z^2(\boldsymbol{\rho}')S_z^2(\boldsymbol{\rho}''), \tag{14}$$

with

$$K(\boldsymbol{\rho}) = \int\frac{d^3k}{(2\pi)^3}\frac{k_x^2k_z^2}{k^4}\left[1 - p\frac{k_z^2}{k^2}\right]\exp(-ik_x x - ik_y y). \tag{15}$$

Changing the order of integration in Eq. (14) one can write it as

$$M_S = \rho\left(\frac{A}{\mu}\right)^2 d^2\int\frac{d^3k}{(2\pi)^3}\frac{k_x^2k_z^2}{k^4}\left[1 - p\frac{k_z^2}{k^2}\right]f(k_\perp), \tag{16}$$

where $k_\perp = \sqrt{k_x^2 + k_y^2}$ and

$$f(k_\perp) = \left|\int d^2\rho\, S_z^2(\rho)\exp(i\mathbf{k}_\perp\cdot\boldsymbol{\rho})\right|^2. \tag{17}$$

Its independence on k_z allows one to integrate over k_z in Eq. (16). This leads to

$$M_S = \frac{1}{16\pi}\rho\left(\frac{A}{\mu}\right)^2 d^2\left(1 - \frac{3}{4}p\right)\int_0^\infty dk_\perp k_\perp^2 f(k_\perp). \tag{18}$$

We now have to compute $f(k_\perp)$. Substituting $S_z(\rho) = (\lambda^2 - \rho^2)/(\lambda^2 + \rho^2)$ from Eq. (1) into Eq. (17), we get

$$f(k_\perp) = (8\pi)^2\lambda^4 u^2(k_\perp\lambda), \quad u(q) = -\int_0^\infty dr\, r\frac{r^3 J_0(qr)}{(1+r^2)^2}, \tag{19}$$

where J_0 is the Bessel function. This gives for the mass

$$M_S = 4\pi\rho\left(\frac{A}{\mu}\right)^2\left(1 - \frac{3}{4}p\right)d^2\lambda\int_0^\infty dq\, q^2u^2(q). \tag{20}$$

Here $u(q)$ given by Eq. (19) can be expressed via special functions, which facilitates numerical computation of the integral. The answer yields

$$M_S = 0.787\left(1 - \frac{3}{4}p\right)\left(\frac{A}{\mu}\right)^2\rho\, d^2\lambda. \tag{21}$$

We have double-checked this result by performing a more tedious integration in real space without replacing the layer of thickness d with a δ function. It produces the same answer with the numeric factor given by

$$c = \frac{1}{16\pi}\int d^2\bar{\rho}'\int d^2\bar{\rho}\left[S_z^2(\bar{\boldsymbol{\rho}}' + \bar{\boldsymbol{\rho}}) - S_z^2(\bar{\boldsymbol{\rho}}')\right]^2\frac{2\bar{x}^2 - \bar{y}^2}{\bar{\rho}^5}, \tag{22}$$

where $\bar{\boldsymbol{\rho}} = \boldsymbol{\rho}/\lambda$. This four-dimensional integral reduces to a one-dimensional integral of an awkward elementary function that has a numerical value of 0.785, very close to the factor in Eq. (21). Notice that for the anisotropic magnetoelastic interaction that we have studied, the mass does not depend on the chirality angle γ.

To see how general this result is, consider now isotropic magnetoelastic coupling of the form $Au_{ik}S_iS_k$. Repeating the steps of the previous calculation we obtain for the skyrmion mass

$$M_S = \rho\left(\frac{A}{\mu}\right)^2 d^2\int\frac{d^3k}{(2\pi)^3}\frac{k_x^2}{k^4}\left[|\mathbf{G}|^2 - p\frac{|\mathbf{k}\cdot\mathbf{G}|^2}{k^2}\right], \tag{23}$$

where

$$\mathbf{G} = \int dx\, dy(\mathbf{k}\cdot\mathbf{S})\mathbf{S}\exp(-ik_xx - ik_yy). \tag{24}$$

This calculation requires more effort as it involves all three components of the skyrmion spin field. The final answer reads

$$M_s = c(p,\gamma)\rho\left(\frac{A}{\mu}\right)^2 d^2\lambda, \tag{25}$$

with the numerical factor given by

$$c(p,\gamma) = 4.118 + 0.727\cos(2\gamma) - p[1.612 + 0.795\cos(2\gamma) + 0.255\cos(4\gamma)]. \tag{26}$$

Thus, in general, one should expect the skyrmion mass to depend on both the elastic properties of the crystal and the chirality of the skyrmion.

The majority of materials have $p \sim 1$. At $p = 1$ one obtains from Eq. (26) $c = 2.186$ for the Néel skyrmion ($\gamma = 0$) and $c = 2.316$ for the Bloch skyrmion ($\gamma = \pi/2$). Notice that this factor for the anisotropic magnetoelastic coupling at $p = 1$ is 0.197, which is an order of magnitude smaller. Up to that factor the proportionality of the skyrmion mass to $\rho(A/\mu)^2d^2\lambda$ is robust. The model correctly captures universal scaling of the mass as the square of the strength of the magnetoelastic coupling, the square of the thickness of the ferromagnetic layer, and the first power of the lateral size of the skyrmion. Notice that the proportionality of the skyrmion phonon mass to its size instead of its volume ($V \sim d\lambda^2$) is related to the fact that only spin-field derivatives contribute to the effect. If a thin-wall skyrmion bubble (or a cylindrical domain) of radius R were considered instead, the mass would have been proportional to the area of the wall and would scale linearly with R.

In a homogeneous system the mass of the skyrmion is determined by the magnetoelastic interaction and the shape of the skyrmion which for small skyrmions is dominated by the exchange. We computed it rigorously for an arbitrary skyrmion size λ in the lowest order on the magnetoelastic interaction. In practice, the size of the skyrmion is determined by the interplay between Dzyaloshinskii-Moriya, crystal-field, and Zeeman interactions. However, in the leading order, these interactions do not contribute to the skyrmion mass.

To estimate the magnitude of the effect, notice that the magnetoelastic energy density A is of relativistic origin (it often comprises a noticeable part of the magnetocrystalline anisotropy), while the shear modulus μ is of electrostatic origin arising from the coupling between atoms in a crystal. This allows one to roughly estimate the ratio A/μ to be in the ballpark of 10^{-4}. At $\rho \sim 5\times 10^3$ kg/m^3 and $d \sim 2$ nm it gives M_S of the order of a few electron masses for a skyrmion of size $\lambda \sim 10$ nm. However, in materials with high magnetostriction this mass can be significantly greater as it scales as the square of the strength of the magnetoelastic coupling.

Note that, in principle, the addition of the magnetoelastic term to the energy of the skyrmion, determined in our model by the exchange constant J, results in the perturbation of the skyrmion shape, which adds corrections to the shape given by Eq. (1). Adding the exchange energy density, $\frac{1}{2}J(\partial_i\mathbf{S}\cdot\partial_i\mathbf{S})$, to Eq. (3) it is easy to see with the help of Eq. (4) that these corrections are negligible as long as the size of the skyrmion is small compared to $(\sqrt{J\mu}/A)a$ (with a being the lattice spacing), which would be typically in the micrometer range. For a nanoscale skyrmion the corresponding modification of our result for the mass is negligible too. We have not included thermal phonons into our consideration. They enter the problem trivially through the independently measurable temperature dependence of elastic and magnetoelastic constants, $\mu(T)$, $\sigma(T)$, and $A(T)$.

The inertial mass enters the kinetic term in the Thiele equation that describes the motion of skyrmions under the action of the external force. It determines the characteristic frequency (see, e.g., Ref. [25]), $\hbar/(M_Sa^2)$, of the oscillating motion of the skyrmion when it is manipulated by, e.g., the magnetic field gradient or a spin-polarized electric current. A common source of the skyrmion mass considered in literature is a confining potential. Without it the translational invariance makes the mass of the skyrmion zero [29] unless one takes into account the always present magnetoelastic interaction, as we did in this Rapid Communication. When it is weak and the skyrmion is small, its inertial mass is small too and the characteristic frequency is too high to be of any concern for applications of skyrmions as memory units. However, in materials with high magnetostriction it can easily be in the upper gigahertz range, thus imposing a practically important limit on the speed of a skyrmion-based computer.

Our results on the scaling of the inertial mass on the strength of the magnetoelastic coupling, skyrmion size, and the thickness of the film must stand for antiskyrmions and for other similar topological spin objects such as antiferromagnetic skyrmions, merons, etc. Using the framework proposed in this Rapid Communication one can develop a software package for obtaining masses of such objects in homogeneous materials with arbitrary crystal symmetry and arbitrary structure of the magnetoelastic coupling.

This work has been supported by Grant No. DE-FG02-93ER45487 funded by the U.S. Department of Energy, Office of Science.

[1] A. A. Belavin and A. M. Polyakov, Metastable states of two-dimensional isotropic ferromagnets, Pis'ma Zh. Eksp. Teor. Fiz. **22**, 503 (1975) [JETP Lett. **22**, 245 (1975)].

[2] D. C. Wright and N. D. Mermin, Crystalline liquids: The blue phases, Rev. Mod. Phys. **61**, 385 (1989).

[3] S. L. Sondhi, A. Karlhede, S. A. Kivelson, and E. H. Rezayi, Skyrmions and the crossover from the integer to fractional quantum Hall effect at small Zeeman energies, Phys. Rev. B **47**, 16419 (1993).

[4] M. Stone, Magnus force on skyrmions in ferromagnets and quantum Hall systems, Phys. Rev. B **53**, 16573 (1996).

[5] A. Bogdanov and A. Hubert, Thermodynamically stable magnetic vortex states in magnetic crystals, J. Magn. Magn. Mater. **138**, 255 (1994).

[6] J. Ye, Y. B. Kim, A. J. Millis, B. I. Shraiman, P. Majumdar, and Z. Tesanovic, Berry Phase Theory of the Anomalous Hall Effect: Application to Colossal Magnetoresistance Manganites, Phys. Rev. Lett. **83**, 3737 (1999).

[7] U. Al'Khawaja, and H. T. C. Stoof, Skyrmions in a ferromagnetic Bose-Einstein condensate, Nature (London) **411**, 918 (2001).

[8] T. H. R. Skyrme, A non-linear theory of strong interactions, Proc. R. Soc. London, Ser. A **247**, 260 (1958).

[9] A. M. Polyakov, *Gauge Fields and Strings* (Harwood Academic, Reading, UK, 1987).

[10] N. Manton and P. Sutcliffe, *Topological Solitons* (Cambridge University Press, Cambridge, UK, 2004).

[11] E. Braaten and L. Carson, Deuteron as a toroidal skyrmion, Phys. Rev. D **38**, 3525 (1988).

[12] W. Y. Crutchfield, N. J. Snyderman, and V. R. Brown, Deuteron in the Skyrme Model, Phys. Rev. Lett. **68**, 1660 (1992).

[13] A. P. Malozemoff and J. C. Slonczewski, *Magnetic Domain Walls in Bubble Materials* (Academic, New York, 1979).

[14] T. H. O'Dell, *Ferromagnetodynamics: The Dynamics of Magnetic Bubbles, Domains, and Domain Walls* (Wiley, New York, 1981).

[15] N. Nagaosa and Y. Tokura, Topological properties and dynamics of magnetic skyrmions, Nat. Nanotechnol. **8**, 899 (2013).

[16] X. Zhang, M. Ezawa, and Y. Zhou, Magnetic skyrmion logic gates: Conversion, duplication and merging of skyrmions, Sci. Rep. **5**, 9400 (2015).

[17] G. Finocchio, F. Büttner, R. Tomasello, M. Carpentieri, and M. Klaui, Magnetic skyrmions: From fundamental to applications, J. Phys. D: Appl. Phys. **49**, 423001 (2016).

[18] A. O. Leonov, T. L. Monchesky, N. Romming, A. Kubetzka, A. N. Bogdanov, and R. Wiesendanger, The properties of isolated chiral skyrmions in thin magnetic films, New J. Phys. **18**, 065003 (2016).

[19] W. Jiang, G. Chen, K. Liu, J. Zang, S. G. E. te Velthuis, and A. Hoffmann, Skyrmions in magnetic multilayers, Phys. Rep. **704**, 1 (2017).

[20] A. Fert, N. Reyren, and V. Cros, Magnetic skyrmions: Advances in physics and potential applications, Nat. Rev. Mater. **2**, 17031 (2017).

[21] G. Yu, P. Upadhyaya, Q. Shao, H. Wu, G. Yin, X. Li, C. He, W. Jiang, X. Han, P. K. Amiri, and K. Wang, Room-temperature skyrmion shift device for memory application, Nano Lett. **17**, 261 (2016).

[22] W. Legrand, D. Maccariello, N. Reyren, K. Garcia, C. Moutafis, C. Moreau-Luchaire, S. Collin, K. Bouzehouane, V. Cros, and A. Fert, Room-temperature current-induced generation and motion of sub-100 nm skyrmions, Nano Lett. **17**, 2703 (2017).

[23] C. Back, V. Cros, H. Ebert, K. Everschor-Sitte, A. Fert, M. Garst, Tianping Ma, S. Mankovsky, T. L. Monchesky, M. Mostovoy, N. Nagaosa, S. S. P. Parkin, C. Peiderer, N. Reyren, A. Rosch, Y. Taguchi, Y. Tokura, K. von Bergmann, and Jiadong Zang, The 2020 skyrmionics roadmap, J. Phys. D: Appl. Phys. **53**, 363001 (2020).

[24] W. Döring, Mikromagnetismus, in *Handbuch Der Physik*, edited by S. Flügge (Springer, Berlin, Heidelberg, 1966), Vol. 18/2, pp. 314–437.

[25] I. Makhfudz, B. Kruger, and O. Tchernyshyov, Inertia and Chiral Edge Modes of a Skyrmion Magnetic Bubble, Phys. Rev. Lett. **109**, 217201 (2012).

[26] F. Büttner, C. Moutafis, M. Schneider, B. Krüger, C. M. Günther, J. Geilhufe, C. v. Korff Schmising, J. Mohanty, B. Pfau, S. Schaffert, A. Bisig, M. Foerster, T. Schulz, C. A. F. Vaz, J. H. Franken, H. J. M. Swagten, M. Klüui, and S. Eisebitt, Dynamics and inertia of skyrmionic spin structures, Nat. Phys. **11**, 225 (2015).

[27] T. Shiino, K.-J. Kim, K.-S. Lee, and B.-G. Park, Inertia-driven resonant excitation of a magnetic skyrmion, Nat. Sci. Rep. **7**, 13993 (2017).

[28] S.-Z. Lin, Dynamics and inertia of a skyrmion in chiral magnets and interfaces: A linear response approach based on magnon excitations, Phys. Rev. B **96**, 014407 (2017).

[29] C. Psaroudaki, S. Hoffman, J. Klinovaja, and D. Loss, Quantum Dynamics of Skyrmions in Chiral Magnets, Phys. Rev. X **7**, 041045 (2017).

[30] V. P. Kravchuk, D. D. Sheka, U. K. Rößler, J. van den Brink, and Y. Gaididei, Spin eigenmodes of magnetic skyrmions and the problem of the effective skyrmion mass, Phys. Rev. B **97**, 064403 (2018).

[31] Z.-X. Li, C. Wang, Y. Cao, and P. Yan, Edge states in a two-dimensional honeycomb lattice of massive magnetic skyrmions, Phys. Rev. B **98**, 180407(R) (2018).

[32] Y. Liu and Z. Liang, Measurement of skyrmion mass by using simple harmonic oscillation, J. Magn. Magn. Mater. **500**, 166382 (2020).

[33] U. K. Rößler, N. Bogdanov, and C. Pfleiderer, Spontaneous skyrmion ground states in magnetic metals, Nature (London) **442**, 797 (2006).

[34] S. Heinze, K. von Bergmann, M. Menzel, J. Brede, A. Kubetzka, R. Wiesendanger, G. Bihlmayer, and S. Blugel, Spontaneous atomic-scale magnetic skyrmion lattice in two dimensions, Nat. Phys. **7**, 713 (2011).

[35] O. Boulle, J. Vogel, H. Yang, S. Pizzini, D. de Souza Chaves, A. Locatelli, T. O. Mentes, A. Sala, L. D. Buda-Prejbeanu, O. Klein, M. Belmeguenai, Y. Roussigné, A. Stahkevich, S. M. Chérif, L. Aballe, M. Foerster, M. Chshiev, S. Auffret, I. M. Miron, and G. Gaudin, Room-temperature chiral magnetic skyrmions in ultrathin magnetic nanostructures, Nat. Nanotechnol. **11**, 449 (2016).

[36] A. Derras-Chouk, E. M. Chudnovsky, and D. A. Garanin, Quantum collapse of a magnetic skyrmion, Phys. Rev. B **98**, 024423 (2018).

[37] L. D. Landau and E. M. Lifshitz, *Theory of Elasticity* (Pergamon, Oxford, New York, 1986).